Block Copolymer/Homopolymer Mesoblends: Preparation and Characterization

Rebecca L. Roberge,[†,§] Nikunj P. Patel,[†] Scott A. White,[∥,#] Wiriya Thongruang,[‡,¶] Steven D. Smith,[⊥] and Richard J. Spontak*[,†,‡]

Departments of Chemical Engineering and Materials Science & Engineering, North Carolina State University, Raleigh, North Carolina 27695, Medical Device Technologies Department, Becton Dickinson Technologies, Research Triangle Park, North Carolina 27709, and Corporate Research Division, The Procter & Gamble Company, Cincinnati, Ohio 45239

Received September 5, 2001

ABSTRACT: Miscible block copolymer/homopolymer blends are typically prepared from homogeneous solutions in a nonselective solvent. During solvent removal and subsequent annealing, the molecular species comprising such blends organize in such fashion as to lower the system free energy and ideally attain thermodynamic equilibrium. In this work, we investigate nonequilibrium triblock copolymer/homopolymer (ABA/hB) blends generated by diffusing hB molecules from a hB-selective solvent into a lamellar ABA copolymer. Since the copolymer is already microphase-ordered during homopolymer incorporation, we refer to such blends as *mesoblends*. The mass uptake of hB is found to be strongly dependent on homopolymer molecular weight (M_{hB}), with the maximum solubility scaling as M_{hB}^{-1}. An induction period that scales as $M_{hB}^{1/2}$ is also observed. Transmission electron microscopy reveals that the morphology of these mesoblends appears to be perforated lamellar, which, in some cases, transforms to cylindrical upon annealing. Dynamic mechanical analysis and differential scanning calorimetry confirm that the A-rich microdomains in the mesoblends are plasticized. The mechanical properties of these mesoblends can be improved upon annealing, but nonetheless differ from those of composition-matched conventional blends.

I. Introduction

Self-organizing block copolymers continue to receive much attention due to their ability to spontaneously form ordered nanostructures.[1] These nanostructures include A(B) spheres or cylinders arranged on a body-centered cubic or hexagonal lattice, respectively, in a B(A) matrix, bicontinuous channels, and lamellae, depending primarily on molecular composition/architecture, thermodynamic incompatibility, and monomer asymmetry.[2] Control over the thermal behavior, morphological features, and bulk properties of these copolymers can be achieved by chemical means, which normally requires tailored synthesis of application-specific copolymer molecules. Alternatively, the characteristics of a microphase-ordered block copolymer can be systematically modified through physical blending with either a (non)preferential solvent,[3,4] a parent homopolymer[5−10] or a second copolymer.[11−15] Of particular interest in the present work is the use of a parent homopolymer to alter the morphology and properties of linear block copolymers. In this case, a fundamental understanding of chain packing within a molecularly confined environment is required to ensure that the added molecules are fully incorporated within the host microdomains of the copolymer to avoid macrophase separation. Previous experimental[5−9] and theoretical[16−18] studies have elucidated molecular design criteria by which to produce miscible diblock copolymer/homopolymer (AB/hB) blends. Similar results have been reported[19,20] for analogous triblock copolymer/homopolymer (ABA/hB) blends, which can form molecular networks due to the existence of B midblocks that form bridges between adjacent A microdomains. Two crucial points must be considered in the design of miscible block copolymer/homopolymer blends: the molecular weight of homopolymer *i* (M_{hi}, i = A or B) relative to that of the *i*th copolymer block (M_i), and the composition of the blend (expressed here in terms of the homopolymer mass percent, w_{hi}). Miscibility is usually retained in such blends if M_{hi}/M_i and w_{hi} are relatively small. An increase in either or both of these quantities ultimately induces macrophase separation at equilibrium.

Equilibrium thermodynamic principles are often invoked[16−18,20] to describe the phase behavior and morphological features of block copolymer/homopolymer melts due to the manner by which such conventional blends are typically produced. Generally speaking, the blend constituents are co-dissolved in, and cast from, a nonselective (common) solvent. Resultant films are subjected to post-annealing to ensure complete solvent removal and promote nanostructural refinement as the system seeks to reach thermodynamic equilibrium. Addition of homopolymer molecules to a microphase-ordered block copolymer in this fashion either swells the host microdomains or induces a morphological transformation to a nanostructure with a different interfacial curvature. If the copolymer exhibits the lamellar morphology and the added homopolymer causes lamellar swelling, the homopolymer molecules are predicted[16−18,20] to locate along the lamellar midplane. The extent to which such localization occurs increases with increasing M_{hi}/M_i.

* To whom correspondence should be addressed.
† Department of Chemical Engineering, North Carolina State University.
‡ Department of Materials Science & Engineering, North Carolina State University.
§ Present address: Oral Care Division, The Procter & Gamble Company, Mason, OH 45040.
∥ Becton Dickinson Technologies.
⊥ The Procter & Gamble Company.
Present address: Global Research and Development, Armacell LLC, Mebane, NC 27302.
¶ Present address: Department of Mechanical Engineering, Prince of Songkhla University, Hatyai, Songkhla 90112, Thailand.

10.1021/ma0115747 CCC: $22.00
Published on Web 02/05/2002

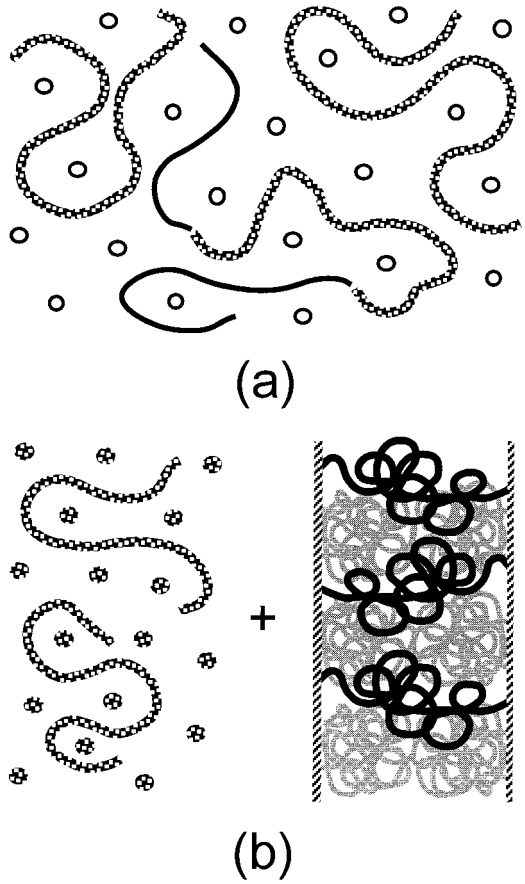

Figure 1. Schematic diagram illustrating the different starting points by which (a) conventional blends and (b) mesoblends are prepared from a microphase-ordered (lamellar) ABA triblock copolymer and homopolyB. In part a, all the blend constituents are co-dissolved in and cast from a common solvent (open circles). In the case of a mesoblend (b), the ordered block copolymer is immersed in a B-selective solvent (speckled circles) containing dissolved homopolyB. Depicted in (b) is a single B lamella composed of both looped and bridged B midblocks (light and dark lines, respectively).

Addition of hB to a lamellar ABA triblock copolymer has a pronounced effect on both nanostructural dimensions and mechanical properties, the latter of which reflects a marked reduction in the fraction of bridged midblocks.[20] Similar results are obtained when a midblock-selective solvent is added to an ABA copolymer to form a gel.[4] We have previously shown[21] that diffusion of such a solvent into the preexisting morphology of a lamellar ABA copolymer results in the formation of *mesogels*, a term originally coined by Halperin and Zhulina,[22] with improved mechanical properties. In the present work, this strategy of diffusing a block-selective additive into a block copolymer nanostructure is used to produce nonequilibrium ABA/hB blends, which we hereafter refer to as *mesoblends*. A schematic diagram illustrating the difference by which mesoblends and conventional blends are prepared is provided in Figure 1. Several series of mesoblends, differing in homopolymer molecular weight and composition, are prepared for investigation in this study. Their mass-uptake and thermal properties are analyzed by gravimetric analysis and differential scanning calorimetry, respectively, whereas the mechanical properties of these mesoblends are measured by dynamic mechanical analysis. Transmission electron microscopy is employed to ascertain the effect of hB incorporation on the lamellar morphology of the ABA copolymer, also before and after annealing.

II. Experimental Section

A. Materials. The same poly(styrene-*b*-isoprene-*b*-styrene) (SIS) triblock copolymer employed in an earlier study[20] of conventional triblock copolymer/homopolymer blends was used to generate the mesoblends in this work for comparative purposes. The copolymer was synthesized via living anionic polymerization in the presence of *sec*-butyllithium. Its number-average molecular weight ($\bar{M}_n$) and polydispersity index (PDI) were 111 000 and 1.04, respectively, and its composition was 54 wt % S. Five homopolyisoprenes with $\bar{M}_n$ of 1000, 7500, 15 000, 30 000, and 60 000 were also synthesized via living anionic polymerization and possessed PDI values less than 1.04. These homopolyisoprenes are hereafter designated as hI*n*, where *n* is an integer given by $\bar{M}_n$/1000. Toluene and *n*-hexane (H) were purchased from Aldrich Chemicals (Milwaukee, WI) and used as-received.

B. Methods. The SIS copolymer was dissolved in toluene to form a 4% w/v solution, which was cast into Teflon molds and allowed to dry slowly over the course of 3 weeks. Resultant films measuring ca. 0.4 mm thick were annealed at 105 °C for 1 h to remove residual solvent and promote nanostructural refinement. The dried films were cut into small squares measuring 1.3 cm × 1.3 cm and weighed. Each homopolyisoprene was dissolved in *n*-hexane (H) at a concentration of 5% w/w. Each hI*n*/H solution (40−50 mL) was placed in a capped Erlenmeyer flask, into which a square of the SIS copolymer was suspended and permitted to swell quiescently at 25 °C. After a given sorption time (t_s), the copolymer film was removed, washed gently in a detergent solution and two successive distilled water baths to remove excess hI*n*, and then dried for 48 h under vacuum at ambient temperature to remove H from the swollen I microdomains. Mass reduction accompanying solvent removal during vacuum-drying was monitored in some cases with a Cahn electrobalance operated at ca. 630 Pa. Control specimens were likewise prepared by exposing the SIS copolymer to H alone. Mesoblend and control films were annealed under vacuum for 7 h at 110 °C (above the glass transition temperature, T_g, of the S endblocks in the copolymer) and reweighed to ascertain the mass of hI*n* sorbed into the copolymer and the solubility of H in the S microdomains.

Differential scanning calorimetry (DSC) of the mesoblends and control specimens was performed under a nitrogen atmosphere with a Perkin-Elmer DSC7 unit. The heating rate was constant at 20 °C/min, and only the first heating cycle was recorded (due to evolution and removal of H vapor during heating). The mechanical properties of the mesoblend and control specimens before and after annealing were examined by dynamic mechanical analysis (DMA), which was conducted with a Rheometrics solids analyzer (RSA-II) operated in tensile mode at 25 °C. Specimen strips measuring 1.3−3.5 cm long and 0.5 cm wide were cut from the treated films, and the dependence of the dynamic storage modulus (E') on frequency (ω) was measured at a strain amplitude of 0.01%, which lies within the linear viscoelastic limit. Specimens for transmission electron microscopy (TEM) were sectioned at −100 °C with a Reichert-Jung Ultracut S ultramicrotome and subsequently stained with the vapor of a 2.0% OsO_4(aq) solution for 90 min. Images of the morphologies in the mesoblends and control specimens before and after annealing were acquired with a Zeiss EM902 electron spectroscopic microscope operated at 80 kV and energy loss settings ranging from 50 to 90 eV. Images were collected on plate film and digitized at 600 dpi prior to analysis with the Digitalmicrograph software package produced by Gatan, Inc. (Pleasanton, CA).

III. Results and Discussion

A. Solvent Considerations. Although micellization of the copolymer molecules in H is not considered

probable due to the presence of a physical network composed of bridged midblocks distributed throughout the copolymer matrix, a major concern in the production of mesoblends is solvent retention. Recall that the mesoblends *cannot* be annealed in the melt without adversely affecting the frozen-in molecular arrangement of the glassy S endblocks. While H serves as a selective solvent for I, it is not a nonsolvent for S. Since the solubility parameters (δ) for H, I, and S are 14.9, 16.6, and 18.7 $MPa^{1/2}$, respectively, the Flory−Huggins (χ) parameters for these nonpolar polymer/solvent pairs are estimated from $0.34 + v_H\Delta\delta^2/RT$ (where v_H is the molar volume of H, $\Delta\delta$ is the difference in δ, R is the universal gas constant, and T denotes absolute temperature) to be about 0.49 for I/H and 1.11 for S/H at 25 °C.[23] Under these conditions, the activity of H (a_H) in the hI*n*/H reservoir is nearly unity and the equilibrium solubility of H in S homopolymer exceeds 10 wt %.[24,25] It is therefore reasonable to expect that the glassy S microdomains of the copolymer are highly plasticized during hI*n* solubilization. In fact, Jacques and Hopfenberg[26] report that the T_g of S homopolymer in pure liquid H is subambient. While the local a_H within the copolymer matrix is most likely less than unity due to the high local concentration of immobilized polymer chains, the diffusion of hI*n* molecules into the I lamellae of the swollen copolymer may be accompanied by the transformation of the S lamellae from glassy to rubbery at ambient temperature. A microphase-separated network nonetheless remains, as evidenced by the mechanical integrity of the highly swollen copolymer films. When the resultant mesoblends are removed and dried, the polymer concentration within the I lamellae increases, while a_H and the equilibrium solubility of H in the S lamellae both decrease. According to prior findings,[24] the T_g of H-plasticized S homopolymer occurs at 25 °C when $a_H \approx 0.75$ and the equilibrium solubility is ~7.4 mg H/100 mg S (which is equivalent to 6.9 wt % H).

Gravimetric measurements conducted on copolymer control films (with no added hI*n*) indicate that removal of H from the swollen I microdomains under vacuum at 25 °C is virtually complete after ca. 200 min, which is significantly less than the drying time adopted in the present procedure (48 h). Thermograms collected from dried control and mesoblend films exhibit endothermic peaks in the vicinity of 68−71 °C, which corresponds to the normal boiling point of H (at 69 °C). Existence of such peaks confirms that residual H is present in these films after vacuum-drying. The concentration of H responsible for these peaks, estimated from the measured enthalpy of vaporization relative to that of pure H (335 J/g), is about 0.64 wt %. Gravimetric analysis reveals that the residual concentration of H in the copolymer after vacuum-drying is closer to 3.4 wt %. If all the H is presumed to locate within the S microdomains, this result corresponds to a solubility of H in S of about 6.3 wt %, in favorable agreement with the data of Kang et al.[24] Since the S microdomains of the SIS copolymer are apparently glassy at 25 °C and are capable of serving as physical cross-links for existing bridged I midblocks, the mesoblends and control films retain their shape-memory capability. It must be kept in mind, however, that the glassy S lamellae of the unannealed mesoblends remain plasticized, which will certainly have a deleterious effect on the mechanical properties, as well as on the morphological characteristics, of these materials.

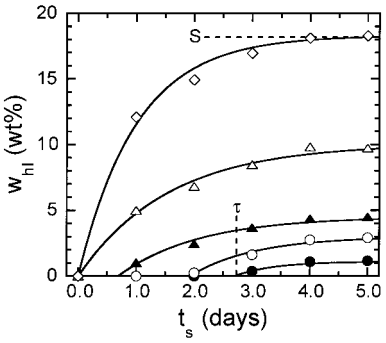

Figure 2. Homopolyisoprene concentration (w_{hI}) presented as a function of sorption time (t_s) for five hI*n* differing in $\bar{M}_n$: 1000 (hI1, ◇), 7500 (hI8, △), 15 000 (hI15, ▲), 30 000 (hI30, ○) and 60 000 (hI60, ●). Examples of the solubility (S) and induction period (τ) are displayed for illustrative purposes. The solid lines correspond to the exponential expression provided in the text.

B. Uptake Kinetics. Immersion of the lamellar SIS copolymer films in the 5% w/v hI*n*/H solutions yields the mass uptake curves displayed in Figure 2. Several key features are evident in this figure. The first and most obvious characteristic is that the extent to which homopolyisoprene is solubilized within the microphase-ordered copolymer (w_{hI}) increases substantially with decreasing M_{hI}. After $t_s = 5.0$ days, for instance, the concentration of incorporated hI60 is only about 1 wt %, whereas that of hI1 exceeds 17 wt %. While the concentrations of solubilized homopolymer differs markedly among the five hI*n* at 5.0 days, this period of time seems to be sufficient to attain the maximum solubility (S) of most of the homopolyisoprenes employed here. [The hI1 uptake remains constant from 5.0 to about 10.0 days and then increases abruptly to >60 wt %, which may reflect a secondary relaxation process or a morphological transition. It is excluded from further analysis here for this reason.]

Another prominent feature visible in Figure 2 is that the time required for the hI*n* molecules to diffuse into the SIS copolymer increases with increasing M_{hI}. Measurable mass increases are recorded for hI1, hI8, and hI15, but not for hI30 and hI60, after $t_s = 1.0$ day. The data presented in Figure 2 strongly suggest that an induction period (τ) exists for three out of the five hI*n* investigated here. Since only a limited number of data points have been collected to discern uptake trends with regard to M_{hI}, we have fitted all the nonzero data in Figure 2 to an exponential expression of the form $S(1 - e^{-\alpha(t_s-\tau)})$ to extract values of S, α, and τ. Both S and τ are displayed as functions of M_{hI} in Figure 3, which clearly shows that S decreases, while τ increases, with increasing M_{hI}. Although it is not provided here, the parameter α also increases (almost linearly) with increasing M_{hI}.

While the data provided in Figure 3 exhibit some scatter, two interesting results can be reasonably identified. The first is that S decreases as M_{hI}^{-1} or, equivalently, N_{hI}^{-1} (where N denotes the number of statistical units along the polymer backbone) increases. If this is so, then the near-constant product SN_{hI} (equal to 1038 wt % hI*n*, with a standard error of less than 6%) provides strong evidence indicating that the total number of hI repeat units solubilized within the I lamellae of the SIS copolymer is bound by an upper limit. Such a limit is most likely dictated by a combination of volume-

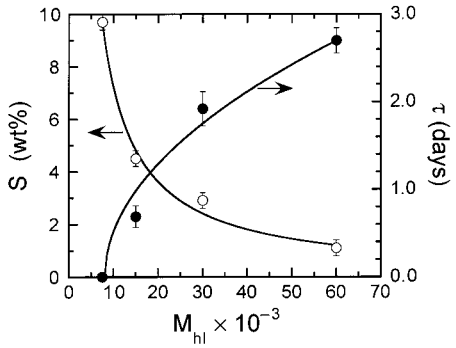

Figure 3. Dependence of S (○) and τ (●) on M_{hI} for four of the homopolyisoprenes examined during the course of this study (hI1 is not included for reasons provided in the text). The solid lines are power-law fits to the data and reveal that $S \sim M_{hI}^{-1}$ and $\tau \sim M_{hI}^{1/2}$. The error bars denote the range of uncertainty in the data derived from the uptake curves presented in Figure 2.

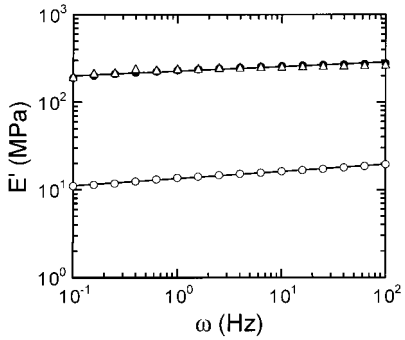

Figure 4. Frequency (ω) spectra of the dynamic storage tensile modulus (E') obtained from the neat SIS triblock copolymer prior to (●) and after (○) exposure to H. Included here are $E'(\omega)$ data collected from the H-plasticized copolymer after annealing at 110 °C for 7 h (△). The solid lines serve to connect the data.

exclusion and physical network considerations (recall that some fraction of the bridged midblocks remains intact and anchored to prevent the copolymer film from losing its mechanical integrity). The other trend evident in Figure 3 is that τ appears to scale as $M_{hI}^{1/2}$. While this relationship is not consistent with any molecular relaxation process from theoretical models describing polymer dynamics in semidilute or concentrated solutions,[27] it does provide insight into the physical mechanism by which homopolymer sorption most likely occurs, as described below.

In 5% w/v solutions, the population of low-M hI molecules is greater than that of high-M hI molecules. For hI molecules to contribute to the measured mass uptake, they must remain at least partially anchored within the copolymer matrix (otherwise, they will be removed during the subsequent cleansing baths). This requirement is more readily satisfied by the low-M hI molecules due to their lower diffusion coefficients. Since the low-M hI molecules are more numerous, can diffuse faster and are less incompatible with respect to the S microdomains in the H-swollen copolymer than the high-M hI molecules, it follows that sorption of homopolymer into the copolymer should occur more quickly in the low-n hIn/H solutions. As M_{hI} increases, however, the time needed for the hI molecules to diffuse sufficiently far into the swollen copolymer and negotiate the loops and bridges within individual lamella, as well as the defects and grain boundaries within the lamellar nanostructure, increases. While τ is therefore intuitively anticipated to increase with increasing M_{hI}, the physical origin responsible for the scaling exponent of $^1/_2$ in $\tau \sim M_{hI}^{1/2}$ is intriguing and warrants further investigation.

C. Mechanical Properties. Recall that the effect of H on the mechanical properties of the SIS copolymer in the absence of added homopolymer is expected to be nontrivial due to H-induced plasticization of the S lamellae. The ω spectrum of E' for the neat SIS copolymer is presented in Figure 4 and reveals that E' is relatively invariant with respect to ω over the three decades of ω explored (from 10^{-1} to 10^2 Hz). Included in this figure is the ω spectrum of E' for a control specimen after exposure to pure H for 1.0 day and subsequent vacuum-drying. Plasticization of the S microdomains is accompanied by a reduction in E' by more than an order of magnitude. Moreover, E' appears to become more ω-dependent. Annealing this plasticized copolymer in the melt (at 110 °C) results in values of E' that are almost identical to those of the neat copolymer before exposure to H. Thus, in the case of the neat SIS copolymer, plasticization of the S microdomains appears to be thermally reversible from the standpoint of mechanical property development, as measured by DMA.

In this section, $E'(\omega)$ data are provided as a function of t_s for several of the vacuum-dried mesoblends examined in this study. Figure 5 displays the ω spectra of E' for mesoblends with hI8 (Figure 5a), hI30 (Figure 5b), and hI60 (Figure 5c). In all cases, the spectrum corresponding to $t_s = 0.0$ days is given by that obtained from the copolymer upon exposure to pure H (see Figure 4). In Figure 5a, E' plummets as t_s, and hence, the concentration of hI8 within the mesoblend increases. A comparable, but less pronounced, decrease in E' is evident in Figure 5b for the SIS/hI30 mesoblend and in Figure 5c for the SIS/hI60 mesoblend. To facilitate comparison of these results, we examine the time dependence of E_t'/E_0, defined as $1/m\sum_{j=1}^{m} E'(\omega_j)/E_0(\omega_j)$, where m is the number of frequencies sampled, ω_j denotes the jth frequency and E_0 corresponds to E' of the vacuum-dried (but not hIn-modified) control copolymer. We use this ratio, rather than the one previously evaluated[20] at 10^{-1} Hz, due to curvature in some of the ω spectra at low ω. Values of E_t'/E_0 are presented for each mesoblend series in Figure 6 and demonstrate (i) that the mechanical response of the SIS/hI30 mesoblend is similar to that of the SIS/hI8 mesoblend at short t_s but closer to that of the SIS/hI60 mesoblend at long t_s and (ii) that the SIS/hI60 mesoblend appears to exhibit an induction period (that is less than τ derived from gravimetric analysis) with regard to its mechanical property development. The noticeable difference in E_t'/E_0 evaluated for the SIS/hI8 and SIS/hI60 mesoblends at long t_s in Figures 5 and 6 is attributed to composition. At $t_s = 5$ days, the concentration of homopolymer in these two mesoblends is about 9.7 and 1.1 wt %, respectively.

The dependence of E' on ω for the SIS/hI15 mesoblend is shown in Figure 7. As in Figure 5, H-assisted incorporation of hI15 into the SIS copolymer results in undesirable plasticization of the S microdomains and promotes a substantial reduction in E' after vacuum-drying. Included in this figure are $E'(\omega)$ data collected from the same mesoblends after annealing to remove residual H. In agreement with the data provided in Figure 4 for the control specimen, annealing is seen to promote an increase in E' by at least an order of magnitude. Note, however, that the values of E'

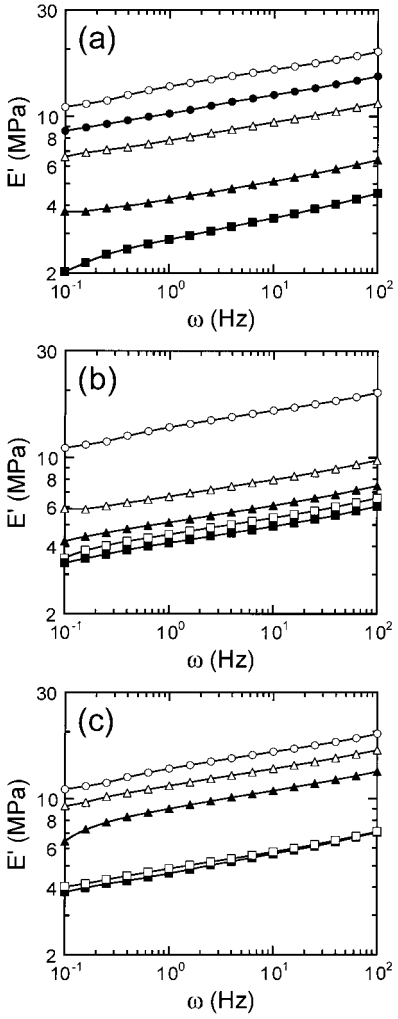

Figure 5. Variation of E' with respect to ω for mesoblends composed of (a) hI8, (b) hI30, and (c) hI60 after exposure to hI*n*/H solutions for different t_s (in days): 0.0 (○), 0.5 (●), 1.0 (△), 2.0 (▲), 3.0 (□), and 5.0 (■). The solid lines serve to connect the data.

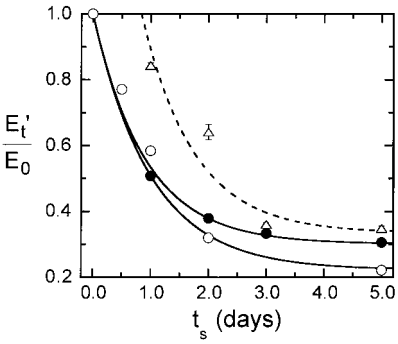

Figure 6. Ratio E_t'/E_0 defined in the text and displayed as a function of t_s for mesoblends prepared with three different homopolyisoprenes: hI8 (○), hI30 (●), and hI60 (△). The solid and dashed lines serve as guides for the eye.

measured from the control specimen after exposure to H, as well as all the mesoblends, exhibit a greater (and similar) dependence on ω compared to the neat SIS copolymer before exposure to H and after annealing (see Figure 4). Rearrangement of the data provided in Figure 7 into the same format as that employed to facilitate comparison in Figure 6 yields the E_t'/E_0 results displayed in Figure 8. While both data sets in this figure indicate that addition of hI15 to the SIS copolymer

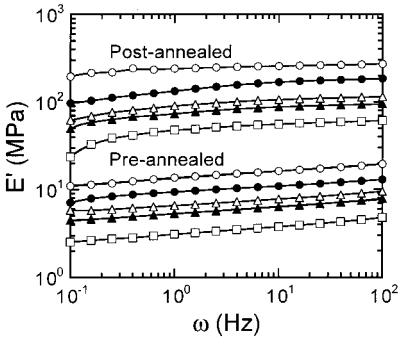

Figure 7. Dependence of E' on ω for SIS/hI15 mesoblends before and after annealing in the melt at 110 °C for different t_s (in days): 0.0 (○), 0.5 (●), 1.5 (△), 2.5 (▲), and 5.0 (□). The solid lines serve to connect the data.

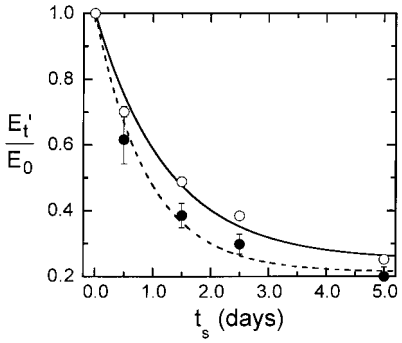

Figure 8. Variation of E_t'/E_0 with respect to t_s for SIS/hI15 mesoblends before (○) and after (●) annealing in the melt at 110 °C. The solid and dashed lines serve as guides for the eye.

softens the material, the relative magnitude of this reduction is marginally greater *after* the mesoblends are annealed. This difference may reflect annealing-induced changes in morphology, as discussed below.

D. Morphological Characteristics. The morphology of the neat SIS copolymer is lamellar with a repeat period (D) of 45.6 nm, as measured[20] from 2D Fourier transforms of digitized TEM images and small-angle X-ray scattering. Assuming the existence of narrow interphases, the average width (L) of the S and I lamellae can be calculated from $\phi_S D$ and $(1 - \phi_S)D$, respectively, where ϕ_S denotes the volume fraction of S (50 vol %) in the copolymer. This analysis yields $L_S = L_I = 22.8$ nm. Since the copolymer has been described and employed elsewhere,[20] we focus our attention here on the mesoblends under current investigation. A montage of TEM images acquired from four mesoblends ($t_s = 6.0$ days) generated with different hI*n* is presented in Figure 9 and reveals that the lamellar morphology of the parent copolymer is not preserved. Instead, an altered lamellar morphology that appears to be highly perforated and, in some instances, discontinuous is evident in each of these images (which are representative of the center regions of the bulk films). Unlike other examples[28] of perforated lamellae (PL) in microphase-ordered block copolymers, the nanostructures seen in these images do not appear to exhibit regular spacing along the perforation normal. Depending on thermal history, however, random perforations can be induced in block copolymer systems undergoing microphase ordering.[29] In some cases, as M_{hI} is increased (see, e.g., the SIS/hI60 mesoblend in Figure 9d), the morphology seems to consist of dispersed, possibly cylindrical, nanostructural elements.

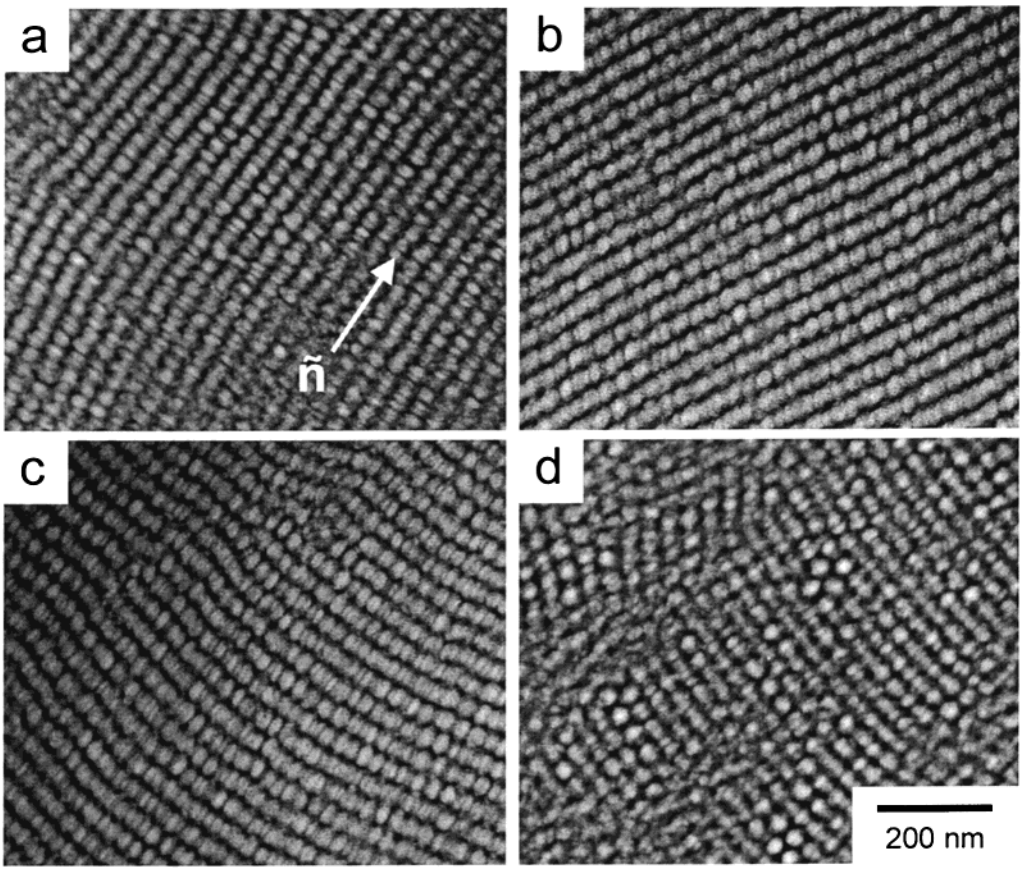

Figure 9. Transmission electron micrographs of SIS/hI*n* mesoblends ($t_s = 6.0$ days) produced with four different hI*n*: (a) hI8, (b) hI15, (c) hI30, and (d) hI60. In all cases, the I microdomains of these mesoblends are electron-opaque (dark) due to selective OsO_4 staining. The director corresponding to the perforation normal, which is perpendicular to the lamellar normal, is identified by $\tilde{n}$ in part a.

It must be recognized that the nonlamellar morphologies visible in Figure 9 do not just reflect the addition of hI*n*. Examination of the control specimens confirms that nonlamellar morphologies similar to those in Figure 9a develop as the result of extended exposure of the copolymer to H. This morphological transformation is attributed to H-induced plasticization of the S microdomains coupled with the development of high interfacial stresses that accompany copolymer swelling. In this vein, it is noteworthy that S homopolymer films exposed to liquid H exhibit evidence of H-induced microvoid formation (crazing) upon swelling.[26] Values of D measured along the PL normal in images such as those shown in Figure 9 are provided as a function of M_{hI} in Figure 10 and indicate that, with the exception of the SIS/hI1 system, the nanostructures in these mesoblends generally exhibit a smaller D relative to that of the parent copolymer. This apparent change in D does not, however, correlate with M_{hI}, as it does in conventional SIS/hI*n* blends.[20] The thicknesses of the S microdomains along the perforation normal (signified by $\tilde{n}$ in Figure 9a) vary from 15.7 ± 1.0 nm in the SIS/hI8 mesoblend (Figure 9a) to 27.8 ± 1.8 nm in the SIS/hI60 mesoblend (Figure 9d). Computation of mesoblend composition from 2D images such as these is virtually impossible due to the complex features present. A more detailed volumetric analysis of these nanostructures by transmission electron microtomography (TEMT)[13,30] is forthcoming. For the same reason, a more detailed analysis of the DMA data by means of the models proposed by Takayanagi et al.[31] or Gray and McCrum[32] for multiphase polymer systems is effectively precluded until the complex morphology of these mesoblends is unambiguously identified.

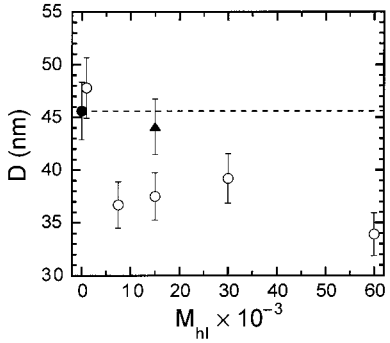

Figure 10. Microdomain repeat period (D, ○) along the lamellar normal derived from TEM images of SIS/hI*n* mesoblends ($t_s = 6.0$ days, see Figure 9) and presented as a function of M_{hI}. Values of D measured from the neat (untreated) SIS copolymer (●), as well as from the annealed SIS/hI15 mesoblend (▲), are included for comparison. The error bars denote the uncertainty in the data, and the dashed line identifies the value of D corresponding to the neat copolymer.

Annealing of the control films after exposure to H and vacuum-drying promotes re-formation of the lamellar morphology in the neat SIS copolymer. The same is not true in the case of the mesoblends. Little morphological change occurs in the SIS/hI30 and SIS/hI60 mesoblends upon annealing at 110 °C for 7 h. Such invariance is attributed to the high M_{hI} of the incorporated homopolymers. At lower M_{hI}, however, morphological changes are observed upon annealing. Figure 11 displays two TEM

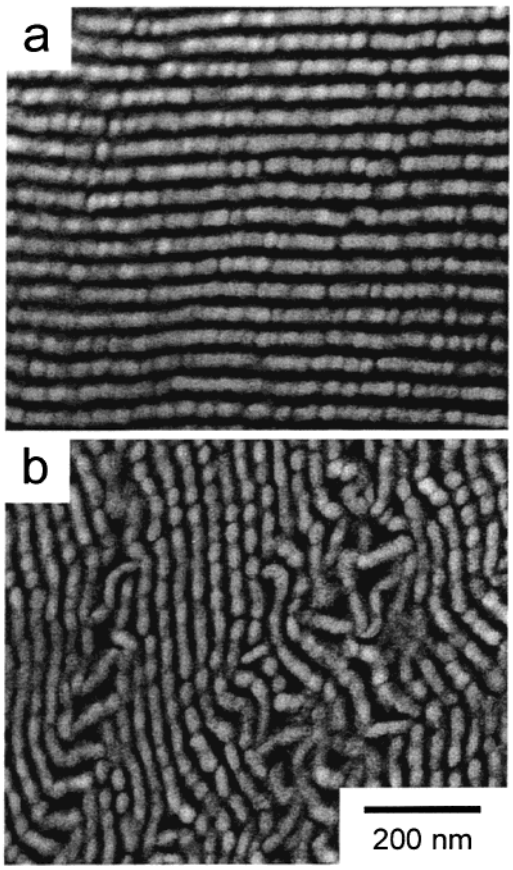

Figure 11. Pair of TEM images acquired from the SIS/hI15 mesoblend (t_s = 5.0 days) after annealing in the melt at 110 °C. The swollen S microdomains evident in Figure 9 are replaced by more continuous lamellae as H is removed from the glassy S microdomains and the melt is driven in the direction of thermodynamic equilibrium.

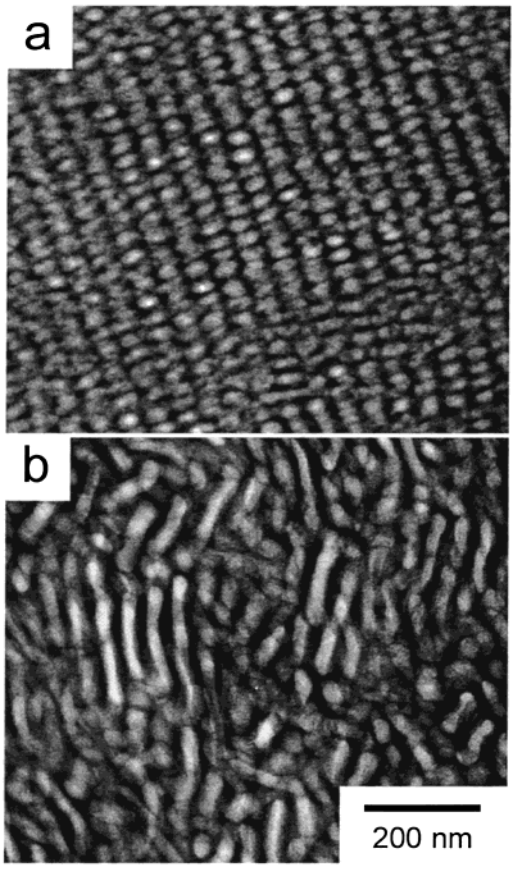

Figure 12. Representative TEM images of the SIS/hI1 mesoblend (t_s = 7.0 days) before and after annealing in the melt at 110 °C (a and b, respectively). The lamellae initially present in the neat SIS copolymer transform into S cylinders dispersed in an I matrix due to the mesoblend composition (W_I = 0.55). At this composition, the nanostructure is expected[20] to adopt a more highly curved morphology as it seeks to reach equilibrium.

micrographs acquired from the annealed SIS/hI15 mesoblend (t_s = 5.0 days). The one shown in Figure 11a reveals the existence of a PL morphology in which the S microdomains appear more continuous and regular, as well as slightly thinner along the lamellar normal (26.3 nm vs 31.6 nm), than in the unannealed analog in Figure 9b. Note also that annealing promotes a ~20% increase in D (see Figure 10). Similar microdomain features, as well as some complex defect structures, are evident in Figure 11b. Further reduction of M_{hI} yields the morphologies of the SIS/hI1 mesoblend (t_s = 7.0 days) before (Figure 12a) and after (Figure 12b) annealing. This pair of images clearly demonstrates that the nonequilibrium PL morphology present in this mesoblend transforms into a cylindrical morphology upon annealing in the melt. It is interesting that the cylinders do not exhibit any evidence of hexagonal arrangement.

E. Blend Comparisons. The morphological transformation seen in Figure 12 is consistent with the bulk composition of the SIS/hI1 mesoblend after t_s = 7.0 days. The concentration of hI1 in this mesoblend is about 18 wt % (see Figure 2), which corresponds to an overall I mass fraction (W_I) of 0.55. While no data are available to describe the phase behavior of conventional SIS/hI1 blends, we draw upon previously reported[20] results obtained from conventional SIS/hI8 blends. In such blends, a transition from lamellar to bicontinuous nanostructure is found to occur in the composition range $0.52 < W_I \leq 0.54$. Since hI1 possesses a lower M_{hI} than hI8 and is therefore able to wet the brushes formed by the I midblocks within the I lamellae more effectively than hI8, the hI1 homopolymer is expected to favor a curved (nonlamellar) morphology in conventional SIS/hI1 blends at W_I = 0.55. The morphological transformation evident in Figure 12 is therefore consistent with the composition-dependent phase behavior of the SIS/hI1 blend as it strives to reach thermodynamic equilibrium upon annealing in the melt. In marked contrast, the hI*n* solubilities provided in Figure 3 correspond to W_I ranging from 0.47 (SIS/hI60) to 0.51 (hI8), all of which lie below the respective blend compositions required to promote a morphological transition from lamellae to bicontinuous channels or cylinders. On the basis of these results, we conclude that annealing all the mesoblends investigated here, except for those in the SIS/hI1 series, will *eventually* restabilize a lamellar morphology that is swollen relative to that of the neat SIS copolymer. As in other metastable PL systems,[33,34] however, the nonequilibrium nanostructures observed in the present mesoblends may be relatively long-lived.

One of the practical motivations for investigating mesoblends is the possibility of producing triblock copolymer/homopolymer blends with superior mechanical properties. A comparison of mechanical properties obtained by DMA from both SIS/hI8 mesoblends and conventional blends (expressed in the form of E_t'/E_0) is provided in Figure 13. It must be remembered that the conventional blends are not plasticized, in which case the absolute magnitudes of E' are at least an order of

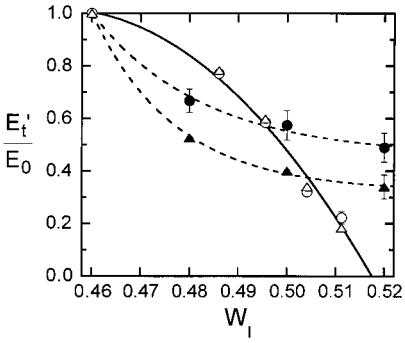

Figure 13. Dependence of E_t'/E_0 on (meso)blend composition (expressed in terms of the overall isoprene mass fraction, W_I) for SIS/hI8 mesoblends (open symbols) and conventional blends (filled symbols). Values of E_t'/E_0 are determined from the definition provided in the text (circles), whereas those calculated at $\omega = 10^{-1}$ Hz (triangles) are included for comparison with results reported earlier[20] for conventional SIS/hI*n* blends. The solid and dashed lines serve as guides for the eye.

magnitude higher than those of the analogous mesoblends. To permit a fair comparison, the values of E_0 used in the present normalization correspond to the neat SIS copolymer (conventional blends) and the vacuum-dried/unannealed SIS copolymer (mesoblends). The results shown in this figure reveal that, relatively speaking, the mesoblends exhibit superior mechanical properties (higher E_t'/E_0) relative to the comparable conventional blends only at low hI concentrations. As the concentration of hI is increased, however, such superiority is clearly no longer achieved.

In addition to blend composition, another point to be considered in such a comparison is M_{hI}. Although not shown here, an increase in M_{hI} shifts the $E_t'/E_0(W_I)$ curve to the left, since less hI is imbibed into the copolymer matrix. This shift reduces the window of opportunity over which the properties of mesoblends can be exploited. Conversely, a decrease in M_{hI} is anticipated to increase the W_I range over which mesoblends exhibit attractive mechanical properties relative to conventional blends. While no experimental data based on hI incorporation into a lamellar SIS copolymer are available to support this claim, we again turn our attention to the subject of mesogels. Mesogels prepared by imbibing an aliphatic mineral oil ($M < 500$) into a lamellar poly(styrene-*b*-(ethylene-*alt*-propylene)-*b*-styrene) triblock copolymer have been found[21] to possess superior mechanical properties (in terms of E') relative to conventional gels over *all* compositions. Although the chemistry and thermodynamics of the two systems clearly differ, the mesogels prepared with a low-M oil serve as a logical extension to the present study. Thus, this previous result is consistent with the expectation discussed above.

IV. Conclusions

The preparation and characterization of triblock copolymer/homopolymer mesoblends have been investigated. Unlike conventional blends that rely on co-dissolution/casting of blend constituents, these mesoblends are produced by exposing an ordered triblock copolymer to a midblock-selective homopolymer solution and permitting migration of homopolymer molecules into the swollen copolymer. The maximum solubility of several (hB) homopolymers into the corresponding lamellae of a lamellar ABA triblock copolymer is found to scale as M_{hB}^{-1}, whereas the induction time observed during homopolymer uptake increases as $M_{hB}^{1/2}$. A more detailed investigation of the kinetics of homopolymer sorption in lamellar block copolymers is currently underway. Dynamic mechanical analysis of the present mesoblends reveals a general reduction in modulus due primarily to solvent-induced plasticization of the glassy microdomains within the copolymer. An increase in the concentration of incorporated homopolymer further lowers the modulus.

Exposure of the neat copolymer to a midblock-selective solvent (e.g., hexane), as well as to homopolymer solutions prepared with this solvent, results in the transformation of lamellae to perforated lamellae, which appear to be further stabilized and/or modified upon addition of homopolymer. Annealing these mesoblends in the melt may promote further morphological transformation to a nonlamellar morphology, depending on mesoblend composition. Comparison of the mechanical properties of mesoblends with respect to those of analogous conventional blends reveals that the mesoblends exhibit a higher normalized modulus at relatively low homopolymer concentrations. This observation is attributed to greater retention of the initial population of bridged midblocks at short exposure times due to (i) a lower concentration of imbibed homopolymer and (ii) a lower probability of chain pullout from the plasticized S lamellae. The results presented here strongly suggest that, by judicious choice of copolymer and selective solvent, it may be possible to systematically produce nonequilibrium copolymer/homopolymer blends with interesting morphological characteristics[35,36] and novel properties.

Acknowledgment. This work was supported, in part, by the U.S. Department of Energy under Contract No. DE-FG02-99ER14991. We thank Ms. E. A. Wilder (NC State) for technical assistance and Prof. H. Hasegawa (Kyoto U.) for valuable advice.

References and Notes

(1) Bates, F. S.; Fredrickson, G. H. *Phys. Today* **1999**, *52*, 32.
(2) Hamley, I. W. *The Physics of Block Copolymers*; Oxford University Press: New York, 1998.
(3) Hanley, K. J.; Lodge, T. P. *J. Polym. Sci., B: Polym. Phys.* **1998**, *36*, 3101. Hanley, K. J.; Lodge, T. P.; Huang, C. I. *Macromolecules* **2000**, *33*, 5918.
(4) Laurer, J. H.; Khan, S. A.; Spontak, R. J.; Satkowski, M. M.; Grothaus, J. T.; Smith, S. D.; Lin, J. S. *Langmuir* **1999**, *15*, 7947.
(5) Winey, K. I.; Thomas, E. L.; Fetters, L. J. *J. Chem. Phys.* **1991**, *95*, 9367. Winey, K. I.; Thomas, E. L.; Fetters, L. J. *Macromolecules* **1991**, *24*, 6182; **1992**, *25*, 2645.
(6) Tanaka, H.; Hashimoto, T. *Macromolecules* **1991**, *24*, 5713. Kimishima, K.; Hashimoto, T.; Han, C. D. *Macromolecules* **1995**, *28*, 3842. Bodycomb, J.; Yamaguchi, D.; Hashimoto, T. *Macromolecules* **2000**, *33*, 5187.
(7) Spontak, R. J.; Smith, S. D.; Ashraf, A. *Macromolecules* **1993**, *26*, 956. Laurer, J. H.; Smith, S. D.; Samseth, J.; Mortensen, K.; Spontak, R. J. *Macromolecules* **1998**, *31*, 4975.
(8) Floudas, G.; Meramveliotaki, K.; Hadjichristidis, N. *Macromolecules* **1999**, *32*, 7496.
(9) Lammertink, R. G. H.; Hempenius, M. A.; Thomas, E. L.; Vancso, G. J. *J. Polym. Sci., B: Polym. Phys.* **1999**, *37*, 1009. Urbas, A.; Fink, Y.; Thomas, E. L. *Macromolecules* **1999**, *32*, 4748. Urbas, A.; Sharp, R.; Fink, Y.; Thomas, E. L.; Xenidou, M.; Fetters, L. J. *Adv. Mater.* **2000**, *12*, 812.
(10) Yang, L. Z.; Gido, S. P.; Mays, J. W.; Pispas, S.; Hadjichristidis, N. *Macromolecules* **2001**, *34*, 4235.
(11) Hashimoto, T.; Yamasaki, K.; Koizumi, S.; Hasegawa, H. *Macromolecules* **1993**, *26*, 2895. Kimishima, I.; Jinnai, H.; Hashimoto, T. *Macromolecules* **1999**, *32*, 2585. Court, F.; Hashimoto, T. *Macromolecules* **2001**, *34*, 2536.

(12) Zhao, J.; Majumdar, B.; Schulz, M. F.; Bates, F. S.; Almdal, K.; Mortensen, K.; Hajduk, D. A.; Gruner, S. M. *Macromolecules* **1996**, *29*, 1204. Koneripalli, N.; Levicky, R.; Bates, F. S.; Matsen, M. W.; Satija, S. K.; Ankner, J.; Kaiser, H. *Macromolecules* **1998**, *31*, 3498.
(13) Spontak, R. J.; Fung, J. C.; Braunfeld, M. B.; Sedat, J. W.; Agard, D. A.; Kane, L.; Smith, S. D.; Satkowski, M. M.; Ashraf, A.; Hajduk, D. A.; Gruner, S. M. *Macromolecules* **1996**, *29*, 4494.
(14) Sakurai, S.; Irie, H.; Umeda, H.; Nomura, S.; Lee, H. H.; Kim, J. K. *Macromolecules* **1998**, *31*, 336.
(15) Goldacker, T.; Abetz, V. *Macromolecules* **1999**, *32*, 5165. Goldacker, T.; Abetz, V. *Macromol. Rapid Commun.* **1999**, *20*, 415. Abetz, V.; Goldacker, T. *Macromol. Rapid Commun.* **2000**, *21*, 16.
(16) Shull, K. R.; Winey, K. I. *Macromolecules* **1992**, *25*, 2637.
(17) Whitmore, M. D.; Vavasour, J. D. *Acta Polym.* **1995**, *46*, 341. Vavasour, J. D.; Whitmore, M. D. *Macromolecules* **2001**, *34*, 3471.
(18) Matsen, M. W. *Phys. Rev. Lett.* **1995**, *74*, 4225; *Macromolecules* **1995**, *28*, 5765.
(19) Lee, S. H.; Koberstein, J. T.; Quan, X.; Gancarz, I.; Wignall, G. D.; Wilson, F. C. *Macromolecules* **1994**, *27*, 3199.
(20) Kane, L.; Norman, D. A.; White, S. A.; Matsen, M. W.; Satkowski, M. M.; Smith, S. D.; Spontak, R. J. *Macromol. Rapid Commun.* **2001**, *22*, 281.
(21) King, M. R.; White, S. A.; Smith, S. D.; Spontak, R. J. *Langmuir* **1999**, *15*, 7886.
(22) Halperin, A.; Zhulina, E. B. *Europhys. Lett.* **1991**, *16*, 337. Zhulina, E. B.; Halperin, A. *Macromolecules* **1992**, *25*, 5730.
(23) Du, Y.; Xue, Y.; Frisch, H. L. In *Physical Properties of Polymers Handbook*; Mark, J. E., Ed.; AIP Press: New York, 1996; Chapter 16.
(24) Kang, Y. S.; Meldon, J. H.; Sung, N. *J. Polym. Sci., B: Polym. Phys.* **1990**, *28*, 1093.
(25) Zielinski, J. M. Unpublished results.
(26) Jacques, C. H. M.; Hopfenberg, H. B. *Polym. Eng. Sci.* **1974**, *14*, 441.
(27) Doi, M.; Edwards, S. F. *The Theory of Polymer Dynamics*; Oxford University Press: Oxford, England, 1988.
(28) Burger, C.; Micha, M. A.; Oestreich, S.; Förster, S.; Antonietti, M. *Europhys. Lett.* **1998**, *42*, 425. Zhu, L.; Huang, P.; Cheng, S. Z. D.; Ge, Q.; Quirk, R. P.; Thomas, E. L.; Lotz, B.; Wittmann, J. C.; Hsiao, B. S.; Yeh, F. J.; Liu, L. Z. *Phys. Rev. Lett.* **2001**, *86*, 6030.
(29) Spontak, R. J.; Alexandridis, P. *Curr. Opin. Colloid Interface Sci.* **1999**, *4*, 140.
(30) Laurer, J. H.; Hajduk, D. A.; Fung, J. C.; Sedat, J. W.; Smith, S. D.; Gruner, S. M.; Agard, D. A.; Spontak, R. J. *Macromolecules* **1997**, *30*, 3938. Jinnai, H.; Nishikawa, Y.; Spontak, R. J.; Smith, S. D.; Agard, D. A.; Hashimoto, T. *Phys. Rev. Lett.* **2000**, *84*, 518. Jinnai, H.; Kajihara, T.; Watashiba, H.; Nishikawa, Y.; Spontak, R. J. *Phys. Rev. E* **2001**, *64*, 10803(R).
(31) Takayanagi, M.; Imada, K.; Kajiyama, T. *J. Polym. Sci. C* **1966**, *15*, 263.
(32) Gray, R. W.; McCrum, N. G. *J. Polym. Sci., A-2: Polym. Phys.* **1969**, *7*, 1329.
(33) Hajduk, D. A.; Takenouchi, H.; Hillmyer, M. A.; Bates, F. S.; Vigild, M. E.; Almdal, K. *Macromolecules* **1997**, *30*, 3788.
(34) Matsen, M. W.; Bates, F. S. *J. Chem. Phys.* **1997**, *106*, 2436. Matsen, M. W.; Thompson, R. B. *J. Chem. Phys.* **1999**, *111*, 7139. Matsen, M. W. *J. Chem. Phys.* **2000**, *113*, 5539.
(35) Lipic, P. M.; Bates, F. S.; Matsen, M. W. *J. Polym. Sci., B: Polym. Phys.* **1999**, *37*, 2229.
(36) Hashimoto, T.; Mitsumura, N.; Yamaguchi, D.; Takenaka, M.; Morita, H.; Kawakatsu, T.; Doi, M. *Polymer* **2001**, *42*, 8477.

MA0115747